Investigating cerebellar control in slow gait adaptations: Insights from predictive simulations of split-belt walking

Sophie Fleischmann[1*], Julian Shanbhag[2], Joerg Miehling[2], Sandro Wartzack[2], Carmichael Ong[3], Bjoern M Eskofier[1,4], Anne D Koelewijn[5],

1 Machine Learning and Data Analytics Lab, Department Artificial Intelligence in Biomedical Engineering (AIBE), Friedrich-Alexander-Universität Erlangen-Nürnberg (FAU), Erlangen, Germany
2 Engineering Design, Department of Mechanical Engineering, Friedrich-Alexander-Universität Erlangen-Nürnberg (FAU), Erlangen, Germany
3 Department of Bioengineering, Stanford University, Stanford, California, USA
4 Translational Digital Health Group, Institute of AI for Health, Helmholtz Zentrum München - German Research Center for Environmental Health, Neuherberg, Germany
5 Chair of Autonomous Systems and Mechatronics, Department of Electrical Engineering, Friedrich-Alexander-Universität Erlangen-Nürnberg (FAU), Erlangen, Germany

* sophie.fl.fleischmann@fau.de

Abstract

During split-belt treadmill walking, neurotypical humans exhibit slow adaptations, characterized by a gradual decrease in step length asymmetry, whereas individuals with cerebellar damage do not show these motor adaptations. We used a neuromusculoskeletal model to better understand individual aspects of the underlying neural control. Specifically, we extended a spinal reflex model by adding a supraspinal layer, representing the cerebellum and its main function of error-driven motor adaptation. The cerebellum, based on the mismatch between an internal prediction and the actual motor outcome, can modulate spinal motor commands within the simulation. Using this model, we investigated the effect of an isolated adaptation of gait timing parameters, in our case the beginning of the liftoff phase. We created 80 s predictive simulations of the model walking on a split-belt treadmill with a 2:1 belt-speed ratio, and evaluated the results by comparing spatiotemporal parameters and kinematics with literature. The simulations exhibited adaptation patterns similar to those observed in human experiments. Specifically, the step length symmetry decreased from an initial asymmetric level toward the baseline, driven primarily by adaptations in the fast step length, while the individual joint kinematics remained similar. The adaptations affected the spatial and temporal domains, represented by a change in the center of oscillation difference and limb phasing. Our findings suggest that reflex gains do not necessarily need to be adapted to achieve changes in step length asymmetry and that, unlike what had been inferred from experiments, the same neural mechanism might account for adaptations in the spatial and temporal domains at different rates. Our simulations demonstrated distinct adaptation patterns corresponding to slow and fast learning behaviors, as reported in the literature, through modifications of a single cerebellar parameter, the adaptation rate. The framework can be extended to test different hypotheses about motor control and adaptations during continuous perturbation tasks.

Author summary

When people walk on a treadmill with the belts running at two different speeds, they initially walk very asymmetrically but gradually decrease certain parameters back toward a symmetric level. We know that the cerebellum is involved in this process, however, the exact neural mechanisms and interdependencies of the numerous interlimb and intralimb adaptation mechanisms remain a topic of ongoing research. We believe that predictive neuromusculoskeletal simulations can advance our understanding of these adaptation processes, as they allow isolating and changing selected arbitrary parameters, which is impossible in human experiments. So far, no models are available in which individual control parameters adapt automatically within the simulation, driven by an embedded physiological process rather than manual adjustments. In our work, we provide a neuromusculoskeletal model extended by a model of the cerebellum, which in turn adapts the gait controller in real-time during the simulation. We found that adapting exclusively the timing of liftoff of the feet can already capture adaptation patterns that are observed in humans with intact cerebellar function. Our model can further be used to test all types of hypotheses about motor adaptation, from adapting individual control parameters to hypotheses about what is stored and adapted during split-belt walking.

Introduction

Humans can effectively adapt their gait in response to perturbations or environmental alterations [1]. From a regulatory perspective, the observed locomotor responses result from an interplay of different neural control processes within the central nervous system. Sudden or unexpected perturbations, such as slips, trigger reactive adaptations characterized by fast corrective muscle activations in response to sensory feedback [2, 3]. Repeated or continuous exposure to perturbations leads to lasting, error-driven modifications of the locomotor pattern that are associated with motor learning [4, 5].

An established paradigm for experimentally inducing both types of locomotor adaptations is split-belt walking, where people walk on a treadmill with the two belts moving at different speeds. Typically, a 2:1 speed ratio is used, with one belt running at 1 m/s and the other at 0.5 m/s [6–10]. Initially, this intervention leads to an immediate adjustment in the gait pattern with noticeable spatiotemporal asymmetries (fast adaptation). However, within several minutes, certain parameters such as the step length or the double support time, gradually readjust toward symmetry (slow adaptation) [6].

Split-belt studies involving patients with cerebellar damage have highlighted the critical role of the cerebellum in the slow adaptation process [11, 12]. Its exact function during motor adaptation is nevertheless a topic of ongoing research. One common hypothesis describes the cerebellum as a forward model whose main functions are sensorimotor prediction and error processing [13]. It generates a prediction of the intended movement outcome based on a stored internal representation, which is then compared to the actual movement outcome [14]. The resulting error leads to a signal that is sent back to the motor cortical and subcortical areas, which activates movement corrections and simultaneously updates the forward model [15, 16]. What exactly this error is, or how the adaptation is carried out, is not yet fully understood.

From a biomechanical standpoint, slow adaptations are characterized by both spatial (foot placement, center of oscillation) and temporal (phasing) adjustments between the limbs [17–19]. Temporal adaptations occur at a faster rate than spatial adaptations, which has led to the assumption that these adjustments are governed by distinct neural mechanisms. Studies focused on muscle activity have further reported adaptations of

activation levels [20] and the temporal structure of activation patterns [21]. Individual joint ranges of motion remain largely unchanged throughout the intervention period [22]. Most studies report the adaptation of interlimb parameters, but adaptations also occur within each limb. These include gradual changes in the absolute stance time as well as the timing of transitions between subphases of the stance phase, particularly in the fast leg. We found, for example, that the duration between the heel strike and start of the liftoff phase gradually increases throughout the intervention (Fig 1). The underlying relationships or causal mechanisms between all observed adaptation processes are difficult to determine through experiments. Recent work has utilized real-time biofeedback to gain further insight into specific control mechanisms, such as the control of limb position or timing [19]. However, in laboratory studies [19], it is impossible to fully isolate and manipulate individual factors to assess their effects [23].

Predictive neuromusculoskeletal simulations are a powerful tool for understanding the contributions of different neural components to motor adaptation because they allow researchers to isolate and alter selected arbitrary components within a system [24]. This capability enables us to investigate how a single component, for example a specific reflex or other control parameter of the model, contributes to motor adaptation, which can improve our overall understanding of the underlying neural control [25]. Simulations can further be used to test the effect of different motor control objectives or hypotheses [23]. Gait simulations with reflex-controlled neuromusculoskeletal models have been shown to be robust against different types of mechanical perturbations, but the perturbations that were applied were almost exclusively perturbations triggering fast adaptation responses [26–28]. In addition, most neuromuscular models focus on the spinal control of walking [29–31]. A few models include supraspinal control structures [32, 33], but they lack essential physiological components, such as the cerebellum, required for the slow motor adaptations observed in split-belt experiments. While in the robotics area, slow adaptations have been reproduced using torque-controlled robots [34, 35], there is only one neuromuscular simulation study focused on slow adaptations in walking. Refy et al. [36] have shown that the adaptation of spinal reflex gains can directly lead to a change in step length asymmetry (SLA). However, the change in reflex was manually induced and not based on any physiological structure.

In this study, we extend a common neuromusculoskeletal reflex model to investigate the mechanisms underlying the slow adaptation processes in split-belt walking that happen during the first minutes of the intervention. Rather than relying on manual manipulation of control parameters, as in [36], we add a realistic supraspinal control structure, specifically a model of the cerebellum. Our cerebellum model mimics the main functions of the human cerebellum, including error-driven motor adaptation, and can independently adapt individual spinal control parameters in a feedforward manner. Theoretically, any spinal control parameter can be modulated by the cerebellum model. Here, we investigate the isolated effect of adapting timing-related parameters of each foot, specifically the timing of the liftoff phase of the gait cycle, while keeping reflex values constant. We generate predictive simulations using single shooting methods to optimize the asymmetric muscle reflex parameters of a gait controller and the cerebellar control parameters for split-belt walking at a 2:1 belt speed ratio. To validate that the simulations capture salient features of motor adaptation, such as the reduction in SLA, we compare spatiotemporal parameters of the simulation results to literature. Then, we elucidate the extent to which the adaptations affect the spatial and temporal domains. Eventually, we use our model to examine the effects of the update rates of the cerebellar internal model and motor commands on step length adaptation.

The contributions of this work thus include the extension of a reflex model by a model of the cerebellum to replicate salient features of motor adaptation, the application of the model to gain insights into the effects of an isolated modulation of

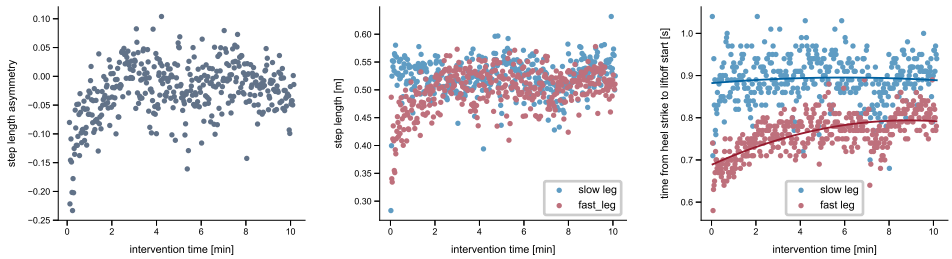

Fig 1. Example of slow adaptations that occur during split-belt walking. Experimentally recorded data from a representative subject walking on a split-belt treadmill with belt speeds of 1 m/s and 0.5 m/s. The left plot shows the progression of step length asymmetry, calculated stride-by-stride from left and right step lengths, which are shown in the middle plot. The right plot displays the time interval between heel strike and liftoff. For details on data recording and computation, refer to S1 File.

timing-related control parameters by the cerebellum, as well as the investigation of the interplay between different cerebellar parameters. Our enhanced model provides a framework to test error metrics of cerebellar learning in motor adaptations and to study the effects of independently adapting different control components which cannot be achieved through human experiments.

Materials and methods

All simulations are conducted in SCONE [38] (version 2.3.1), an optimization and control framework for predictive simulations, and with Hyfydy [39] as the dynamics engine. Our extended model has a hierarchical control structure consisting of a spinal and supraspinal level, which interact with the musculoskeletal system. The spinal layer computes neural muscle excitation signals based on delayed sensory feedback. These excitations are then translated into muscle forces in the musculoskeletal layer using virtual muscle representations. The supraspinal level, representing the cerebellum, continuously adjusts the spinal control based on an error signal while simultaneously updating its internal model. An overview of the approach is given in Fig 2. In the following sections, the different layers are described in more detail together with the treadmill objective function and the optimization protocol.

Musculoskeletal and treadmill model

The sagittal musculoskeletal model is based on the work from Delp [40] with updates from Rajagopal [41]. It is distributed through SCONE and includes a pelvis-trunk segment and two legs, each composed of thigh, shank, and foot. The body segments are connected via six pin joints representing the hip, knee, and ankle joints. A 3-degree of freedom joint between the pelvis and ground allows for translation in the anterior-posterior and vertical directions and for pelvis tilt, resulting in a total of 9 degrees of freedom for the entire model. The lumbar joint is locked at 8.5° of flexion. Each leg is actuated by seven Hill-type muscle-tendon units [42] that represent the major limb muscle groups: hamstrings (HAM), gluteus maximus (GLU), iliopsoas (IL), vasti (VAS), gastrocnemius (GAS), soleus (SOL), and tibialis anterior (TA).

The treadmill model consists of two belts atop the ground. Each belt is modeled as box-shaped contact geometry that could move in the anterior-posterior direction at a predefined speed. Ground reaction forces between the feet and the treadmill belts are

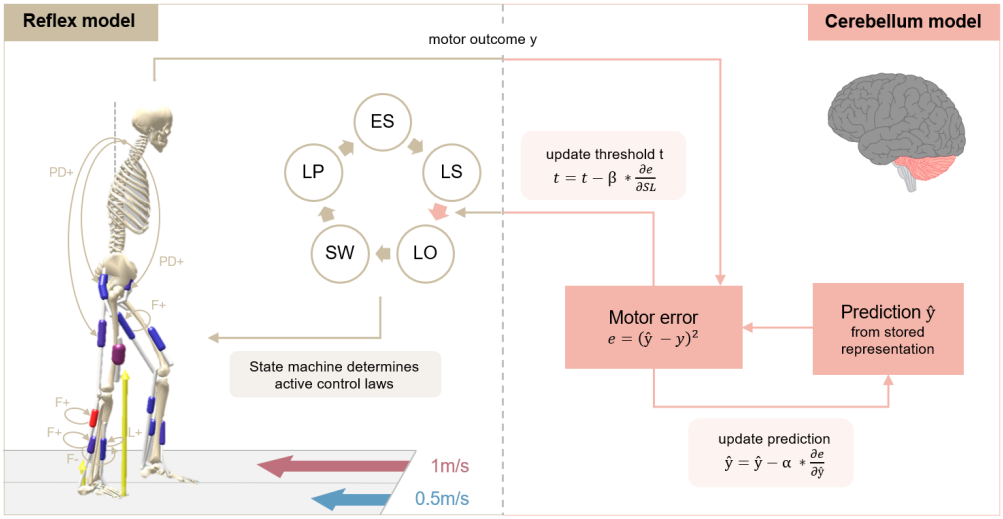

Fig 2. Overview of the spinal and supraspinal control interaction of the extended reflex model. The reflex model has a spinal gait controller based on [37]. A state machine selects the active reflexes based on the current model state, which can be early stance (ES), late stance (LS), liftoff (LO), swing (SW), or landing preparation (LP). The cerebellum compares the motor output y (step length asymmetry in our model) to a predicted output $\hat{y}$, which is generated from an internal representation. Both spinal control and internal predictions are updated based on the partial derivatives of the error with respect to the step lengths SL and to $\hat{y}$, at rates β and α, respectively. In this study, the modulated spinal parameter is the start of the liftoff phase.

computed using the nonlinear Hunt-Crossley contact model [43] and two contact spheres per foot, one at the heel and one at the toes.

Spinal reflex control

The spinal control is based on the reflex-based gait controller from Geyer and Herr [37] (Fig 3). Spinal reflexes translate sensory information into muscle excitation signals via α-motorneurons [37, 44]. Our reflex loops incorporate both muscle force and muscle length information, representing the sensory feedback from the Golgi tendon organs and muscle spindles [44]. The trunk is stabilized with proportional-derivative (PD) control as proposed in [29, 31, 44]. In addition, there are certain constant feedforward muscle excitation signals [37]. The control loops are subject to neural delays that range from 5 ms to 20 ms depending on the distance the signal must travel along the nerves between the muscle and the spinal cord.

Reflexes are generally phase-dependent, meaning they are inhibited or activated during certain periods of the gait cycle [45]. This phase dependency is realized by a state machine that, based on the model's current state, activates selected spinal reflexes. The possible states for each leg correspond to subphases of the gait cycle: early stance (ES), late stance (LS), liftoff (LO), swing (SW), and landing preparation (LP) [29]. The transition between states is based on established thresholds [31, 46, 47] with one modification: Rather than using the contralateral heel strike to trigger the start of the ipsilateral leg's liftoff phase, we introduced an additional threshold t to trigger this transition, where t represents the duration between heel strike and the start of the liftoff phase. While the original transition method is effective for normal walking, we found it insufficient to capture the dynamics of split-belt walking, where alterations in interlimb

	Stance			Swing	
	ES	LS	LO	SW	LP
HAM	PD+, C			F+	
GLU	PD+, C		C	F+	
IL	PD-, C		L+	L+, PD, $L-_{(HAM)}$	
VAS	F+, C				
GAS	F+, C				
SOL	F+, C				
TA	$L+, F-_{(SOL)}$				

Fig 3. The spinal controller consists of different control laws, which are activated based on a state machine. The state machine determines whether the model is in early stance (ES), late stance (LS), liftoff (LO), swing (SW), or landing preparation (LP). Low-level control laws include muscle force feedback (F), muscle length feedback (L), proportional-derivative control based on the pelvis tilt (PD), or a constant signal (C). The (+) and (-) indicate positive and negative feedback. The subscript means that the signal is recieved from the respective muscle, if there is no subscript the feedback law is acted on the same muscle that it is based on.

phasing and limb timing are observed. In our state machine, the transition from late stance to liftoff now occurs after the set time period t following the ipsilateral leg's heel strike.

Cerebellum model

The cerebellum is crucial for motor control and adaptation. It maintains an internal representation of the body dynamics that predicts the outcome of a motor command [14, 48]. When there is a mismatch between the predicted and actual motor outcome, this sensory prediction error is used to adjust the motor signals and simultaneously update its internal model [13, 14]. In this study, we developed a model of the cerebellum capturing key functional aspects that are important for slow adaptations in split-belt walking. It has been hypothesized that the CNS considers interlimb asymmetry an error signal that should be minimized through adaptation [49]. In our model, the cerebellum computes the sensorimotor error e as the squared difference between a predicted and the actual SLA:

$$e = 0.5(\mathrm{SLA}_{\mathrm{pred}} - \mathrm{SLA})^2, \tag{1}$$

where

$$\mathrm{SLA} = \frac{\mathrm{SL_{fast}} - \mathrm{SL_{slow}}}{\mathrm{SL_{fast}} + \mathrm{SL_{slow}}}. \tag{2}$$

During normal walking, this error signal is zero and no motor corrections are made. At the start of the split-belt intervention, the error increases, leading to subsequent movement corrections. $\mathrm{SL_{fast}}$ and $\mathrm{SL_{slow}}$ are the step lengths of the leg on the fast and the slow belt, which are computed as the anterior-posterior distance between both feet at the respective heel strikes (HS) [6]. The calcaneus center of mass (COM) is used to calculate the foot position. The observed SLA is updated after every HS.

The prediction [50], as well as the control signals, are updated based on the error via gradient descent shortly after every HS:

$$\mathrm{SLA_{pred}} = \mathrm{SLA_{pred}} - \alpha \frac{\partial e}{\partial \mathrm{SLA_{pred}}} \tag{3}$$

$$\frac{\partial e}{\partial \mathrm{SLA_{pred}}} = \mathrm{SLA_{pred}} - \mathrm{SLA}, \tag{4}$$

where α is the cerebellar learning rate. In our study, we were interested in adapting only timing-related spinal control signals. Thus, our cerebellum model merely adjusts the timing of the start of the liftoff-off phase of a leg based on the gradient of the sensorimotor error with respect to the step length of the corresponding limb. This is achieved by updating the threshold parameter t of the state machine using the adaptation rate β:

$$t_{\mathrm{slow/fast}} = t - \beta \frac{\partial e}{\partial \mathrm{SL_{slow/fast}}} \tag{5}$$

$$\frac{\partial e}{\partial \mathrm{SL_{slow}}} = \frac{2\mathrm{SL_{fast}}(\mathrm{SL_{slow}} - \mathrm{SL_{fast}} + \mathrm{SLA_{pred}}(\mathrm{SL_{slow}} + \mathrm{SL_{fast}}))}{(\mathrm{SL_{slow}} + \mathrm{SL_{fast}})^3}, \tag{6}$$

$$\frac{\partial e}{\partial \mathrm{SL_{fast}}} = -\frac{2\mathrm{SL_{slow}}(\mathrm{SL_{slow}} - \mathrm{SL_{fast}} + \mathrm{SLA_{pred}}(\mathrm{SL_{slow}} + \mathrm{SL_{fast}}))}{(\mathrm{SL_{slow}} + \mathrm{SL_{fast}})^3}. \tag{7}$$

The cerebellar learning rate α and the adaptation rate β are free controller parameters that are optimized. Unlike the approach in [34], our method enables the individual adaptation of both limbs using a single adaptation rate and a single prediction.

Objective function for treadmill walking

All commonly used objective functions are designed for overground walking, where the ground is stationary and the body moves. These functions cannot be directly applied to treadmill walking, where the COM remains relatively stationary while the treadmill belts move beneath the body. We therefore designed a tiered objective function J, specifically tailored for treadmill walking, which is sought to be minimized:

$$J = \begin{cases} J_t & \text{if } J_t > 0 \\ J_{\mathrm{eff}} + w_{\mathrm{up}} J_{\mathrm{ub}} + J_{\mathrm{dofs}} + w_{\mathrm{pos}} J_{\mathrm{pos}} & \text{if } J_t = 0 \end{cases} \tag{8}$$

All weight factors w_j are shown in Table 1. The primary objective J_t is used to find an initial solution for the model to maintain its position on the treadmill throughout the desired simulation period t_{des} without falling, being dragged backward, or moving forward excessively:

$$J_t = \begin{cases} 0 & \text{if } t_{\mathrm{end}} = t_{\mathrm{des}} \\ \frac{500000}{t_{\mathrm{end}}} & \text{otherwise,} \end{cases} \tag{9}$$

where t_{end} is the total integration time, which continues until the desired simulation time is reached or early stopping is triggered. This happens when the model's vertical COM drops below 85 % of its initial position (indicating that the model has fallen) or when the anterior-posterior pelvis COM deviates more than 10 m from its initial position.

Once this base condition is met ($J_t = 0$), a different set of objective terms is evaluated. It consists of several objectives relevant to human gait in general, and one specifically for treadmill walking, which ensures that the model's COM remains stationary in the global coordinate system. Specifically, J_{eff} minimizes the metabolic rate $\dot{E}$ as defined in [51] and the cubed muscle activations a of the model:

$$J_{\text{eff}} = w_{\text{met}}\dot{E} + w_{\text{act}}\frac{1}{M}\int_0^{t_{\text{end}}}\sum_{i=1}^{M}(a_i^3), \tag{10}$$

where M is the number of muscles and w_{met} and w_{act} are weighting factors. The second term, J_{ub} penalizes excessive upper body motion, by applying a penalty of 100 whenever the absolute pelvis tilt velocity exceeds 10 °/s. J_{dofs} prevents hyperflexion and overextension of the ankle joints by penalizing the respective joint angle α exceeding a range $[\alpha_{\text{min}}\ \alpha_{\text{max}}]$, which was $[-60°, 60°]$ in our case. Additionally, non-physiological knee motions are prevented by minimizing the knee limit torque T caused by the virtual passive knee ligaments [31].

$$J_{\text{dofs}} = w_{\text{ankle}}\int_0^{t_{\text{end}}}(E_{\text{left}}^2 + E_{\text{right}}^2)dt + w_{\text{knee}}\int_0^{t_{\text{end}}}(T_{\text{left}} + T_{\text{right}})dt \tag{11}$$

$$E = \begin{cases} 0 & \text{if } \alpha_{\text{min}} < \alpha < \alpha_{\text{max}} \\ \alpha_{\text{min}} - \alpha & \text{if } \alpha < \alpha_{\text{min}} \\ \alpha - \alpha_{\text{max}} & \text{if } \alpha > \alpha_{\text{max}} \end{cases} \tag{12}$$

Finally, J_{pos} is included in the objective to keep the model in a stationary position, since treadmills have spatial constraints that limit forward or backward movement:

$$J_{\text{pos}} = |\text{COMx}_{\text{HS}_3} - \text{COMx}_{\text{HS}_{\text{end}}}|, \tag{13}$$

where $\text{COMx}_{\text{HS}_3}$ and $\text{COMx}_{\text{HS}_{\text{end}}}$ are the model's anterior-posterior COM position at the third HS and last HS of the same leg, respectively. We used the third instead of the first HS in the objective to allow the model to stabilize first [52].

Table 1. Weight factors of the individual objective terms

w_{ub}	w_{pos}	w_{met}	w_{act}	w_{ankle}	w_{knee}
0.05	100	0.001	20	0.1	0.01

The weight factors were found by trial and error in order to create a realistic and stable-looking walking pattern. Since all objective terms are in different units, a higher weight is not necessarily an indication of higher importance of the respective term.

Generation of split-belt simulations

Our spinal controller was parameterized by 62 muscle control parameters (31 per side) and the left and right threshold parameters t from the state machine. The cerebellum model had two free parameters. The covariance matrix adaptation evolution strategy (CMA-ES) [53] was used to optimize these variables. Similar to other studies, we set the CMA-ES parameters to have a population size λ of 16 and an initial step size σ of

1 [44]. The optimizations terminated either after a maximum number of generations [29] or when the fitness no longer improved, which was the case if the objective function averaged over a window of 500 generations decreased less than $1e-4$ [54, 55]. The initial generalized coordinates and velocities of the model were set, but not optimized. The initial muscle activations were computed by the gait controller, using muscle-tendon lengths and forces obtained through equilibration of the muscle-tendon dynamics based on default minimal activations. The initial muscle states were then determined by re-equilibrating based on the newly computed muscle activations.

To find an initial guess for the muscle reflex parameters of the spinal controller for split-belt walking with a 2:1 belt speed ratio, we generated multiple predictive simulations, starting with both belts running with 1 m/s and gradually reducing the right belt speed to 0.5 m/s in increments of 0.1 m/s. Because the resulting motion did not yet exhibit the same level of asymmetry observed in humans at the start of the split-belt intervention, we manually adjusted some reflex values and reran the optimization with belt speeds set to the 2:1 ratio. Specifically, we adjusted the GAS and SOL force reflex gains during the stance phase, as well as the IL length reflex, because these parameters have been shown to influence step length [44]. By doing so, we created a more asymmetric starting guess for simulating the adaptation period in split-belt walking.

Eventually, we generated twenty 80 s simulations to simulate the adaptation phase of split-belt walking with the left belt running at 1 m/s and the right belt at 0.5 m/s. These specific speeds were chosen based on their frequent use in experimental studies. In human experiments, the adaptation phase typically lasts around five to ten minutes, but due to the high computational complexity of predictive simulations, we limited the maximum duration of our simulations to 80 s. To assess the effect of our cerebellum model, we conducted simulations with and without the cerebellum model. Given the stochastic nature of CMA-ES and the highly nonlinear and non-convex search space [29], we ran ten parallel optimizations for each configuration with the same previously determined initial guess and a maximum of 1500 generations. The first gait cycle of the 80 s simulations was excluded from the analysis [31, 52].

Our cerebellum model is parameterized by the learning rate α and adaptation rate β, where α defines the rate at which the cerebellum's internal prediction is updated, and β determines the extend to which the motor control parameter is updated. To investigate the interplay between the two parameters, we ran 12 additional optimizations. In these, we fixed the adaptation rate to either a low value ($\beta = 0.004$) or a high value ($\beta = 0.04$), while simultaneously setting the initial guess for the learning rate to either a low value ($\alpha = 0.001$) or a high value ($\alpha = 0.025$). The reflex parameters were still optimized. For each of these four combinations, we conducted three parallel optimizations with a maximum 80 s simulation length.

Evaluation

For every simulation, we computed the SLA per stride as the difference between the fast and slow step lengths divided by their sum (see Equation 2). For the simulations with the cerebellum, we additionally decomposed the resulting movements into spatial and temporal components, as proposed by Malone and Bastian [18]. The spatial component, defined as the difference between the centers of oscillation of the fast and slow legs, was calculated stride-by-stride by subtracting the center of oscillation of the fast leg from that of the slow leg. The center of oscillation for each leg was determined as the mean of the limb angle at heel strike and toe-off. In our case, the limb angle was computed as the angle between a vertical line and the vector from the pelvis COM to the calcaneus COM. The temporal component, representing the phasing between the legs, was computed for each stride as the lag time at the peak cross-correlation of the fast and

slow limb angle trajectories, normalized to the stride duration, with the slow leg serving as the reference. For details about the computation, we refer to [18, 56]. The parameters were averaged on a stride-by-stride basis across all respective parallel simulations. The number of strides varied across simulations; therefore, if one simulation had more strides than others, only its final stride was excluded to ensure that averaging across simulations on a stride-by-stride basis always included data from at least two simulations. Finally, the hip, knee, and ankle joint kinematics of the solutions with cerebellum were normalized to the percentage of the stride and averaged across all strides. The code and results of this study are publicly available at `https://simtk.org/projects/splitbelt`, allowing others to replicate our work and build on it.

Results

The model was able to maintain a stable walking pattern for all 80 s simulations and showed adaptation patterns when extended with the cerebellum. Videos of a representative 2:1 split-belt walking simulation, both with and without the cerebellum model, are provided in S2 Video and S3 Video, respectively.

Adaptation of inter- and intralimb gait parameters

Simulations with the cerebellum model demonstrated a gradual adaptation of SLA, starting at -0.14 at the beginning of the intervention and improving to -0.03 by the end (Fig 4). In contrast, when the cerebellum was not included, the step lengths remained asymmetric at around -0.14 throughout the entire simulation period (Fig 5). This behavior is consistent with experimental findings from studies involving both healthy participants and patients with cerebellar damage [11], where patients exhibit an asymmetric gait pattern at the onset of the split-belt intervention but do not show slow adaptations over time. Because we only simulated for 80 s, the change in SLA occurred on a shorter timescale than in experiments, which typically last five to ten minutes. Nevertheless, the adaptation pattern is similar to what is reported in [17, 57], with a high adaptation rate during the first strides followed by a plateau toward the end. In our model, consistent with findings in the literature, the adaptation was primarily driven by changes in the fast leg (Fig 4) where the step length increased [6, 58, 59], in our case from 0.36 m to 0.44 m. Additionally, in our simulations, the step length of the slow leg decreased slightly over the adaptation period, from 0.48 m at the start to 0.46 m at the end, which is also observed in previous work [6, 58, 59].

Spatial and temporal adapatations

To investigate the origins of the change in SLA caused by the isolated modulation of the liftoff threshold by the cerebellum, we decomposed our results into spatial (center of oscillation difference) and temporal (phasing between limbs) components (Fig 6). In humans, both components contribute to slow adaptations but they adapt at different rates, with the temporal adaptation occurring at twice the rate of the spatial adaptation [18]. For us, adapting the liftoff thresholds while keeping all reflex gains constant also resulted in changes in both domains. The simulated center of oscillation difference was higher than reported in [18], but it followed a similar decreasing trend, albeit at a slower rate. Our simulated limb phasing was altered at the beginning of the intervention compared to baseline walking, with the fast leg phase leading the slow leg, and phase shifted back toward baseline level rapidly. This aligns with the results of [18], even though the maximum phase difference is smaller for our model than in experiments.

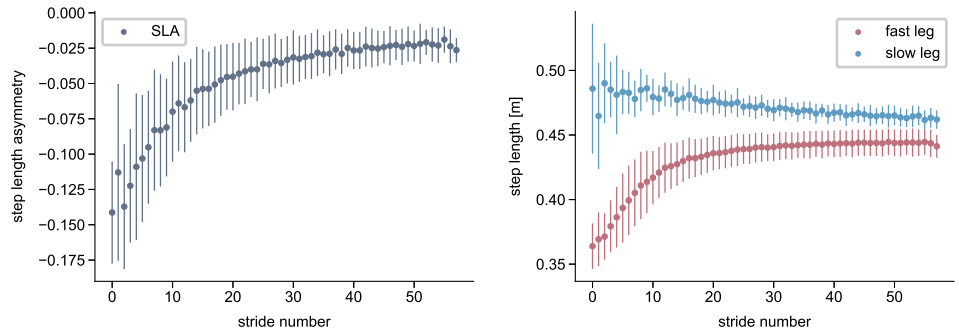

Fig 4. Simulated step length asymmetry and step lengths of the reflex model with the cerebellum during split-belt treadmill walking at a 2:1 speed ratio. All values are averaged over the 80 s simulations, with the bars representing the standard deviation.

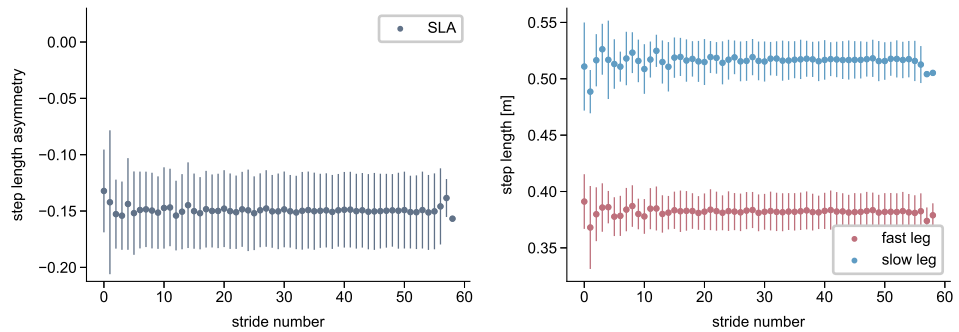

Fig 5. Simulated step length asymmetry and step lengths of the reflex model without the cerebellum (spinal gait controller only) during split-belt treadmill walking at a 2:1 speed ratio. All values are averaged over the 80 s simulations, with the bars representing the standard deviation.

Validity of kinematics

Fig 7 shows the averaged hip, knee, and ankle joint trajectories across all gait cycles from the 80 s simulations with the cerebellar model. In humans, the shift from symmetric walking to split-belt walking induces asymmetries between the kinematics of both limbs, particularly at the ankle joint [60], whereas the kinematics of each joint remain largely unchanged throughout the 2:1 intervention period [22]. This is well reflected by our model, as all kinematic trajectories differed between the fast and slow limb, but showed little adaptation over time, as indicated by the small standard deviation. The simulated kinematic trajectories were not entirely realistic, but did capture some experimentally observed trends [60], particularly for the hip and ankle angles. For instance, the maximum hip extension of the fast leg exceeded that of the slow leg and occurred earlier in the gait cycle, at approximately 50 %, compared to 60 % for the slow leg. At approximately 60 % of the gait cycle, the fast ankle joint was in plantarflexion, while the slow ankle joint was dorsiflexed, which is also observed in human experiments. On the other hand, our simulations exhibited a higher maximum hip flexion than reported in experimental studies, and other parameters, such as the slow ankle range of motion, also deviated from observed data.

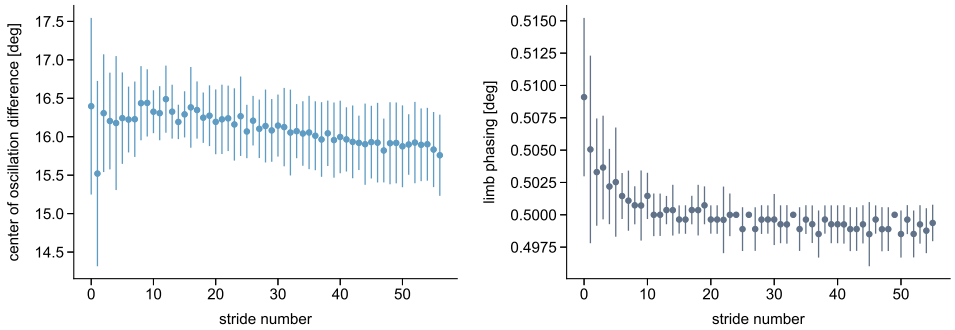

Fig 6. Spatial and temporal adaptation components. The spatial (left plot) and temporal (right plot) components are defined as the center of oscillation difference between the limbs and the interlimb phase, respectively, with the latter computed as the lag time at the peak correlation of each cycle [18]. The baseline values for symmetric walking are 0° for the center of oscillation difference and 0.5 for the limb phasing. The values are averaged over the ten 80 s simulations with the cerebellum, with the bars representing the standard deviation.

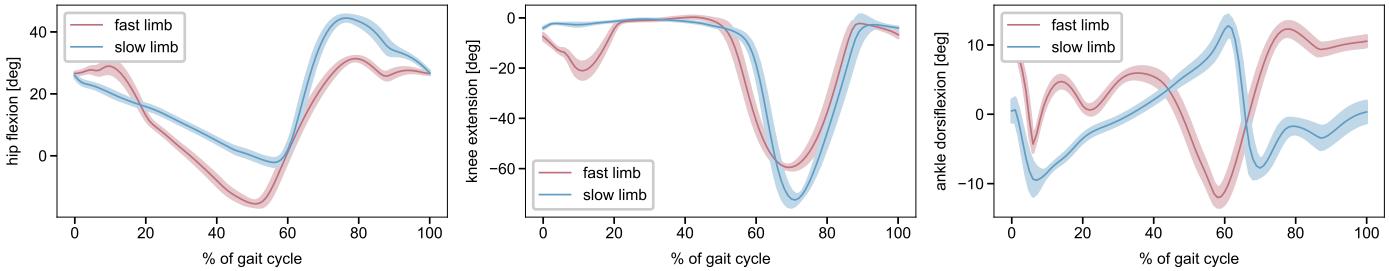

Fig 7. Joint angle trajectories of the hip, knee, and ankle joint during split-belt walking at 2:1 belt-speed ratio. Each gait cycle was normalized to 101 time points. The solid line represents the mean value averaged over all gait cycles resulting from the 80 s simulations with the cerebellum model. The shaded area shows the standard deviation.

Interplay between learning rate and adaptation rate

To assess the interplay between the learning rate and the adaptation rate and their effect on step length adaptation, we conducted additional optimizations by setting the adaptation rate to either a low value ($\beta = 0.004$) or a high value ($\beta = 0.04$), while using a low ($\alpha = 0.001$) or high ($\alpha = 0.025$) initial guess for the learning rate. The resulting SLA curves for each of the four conditions are displayed in Fig 8. In our simulations, both adaptation and learning rate notably influenced the adaptation pattern. A high adaptation rate (blue and green curves) led to a nonlinear change in SLA, characterized by a steep initial rise followed by a plateau towards the end. The learning rate determined the step length symmetry level of this plateau. When the learning rate was high, the SLA reached -0.015 (blue curve), whereas with a low learning rate, it remained lower at -0.08 (green curve). In contrast, a low adaptation rate (red and orange curves) produced a linear adaptation pattern. Here, the learning rate determined the slope of the adaptation curve. A high learning rate resulted in minimal change in SLA (red curve), whereas a low learning rate produced a linear increase without reaching a plateau though. Jacobsen and Ferris [61] have shown that fast and slow adapters exist and that these groups are related to differences in brain activity. The adaptation curves that they found experimentally for fast- and slow-adapting individuals match our results

for high and low adaptation rates with a low learning rate, in the sense that fast learners show a more exponential adaptation curve and reach a steady-state level of SLA with fewer steps than slow learners.

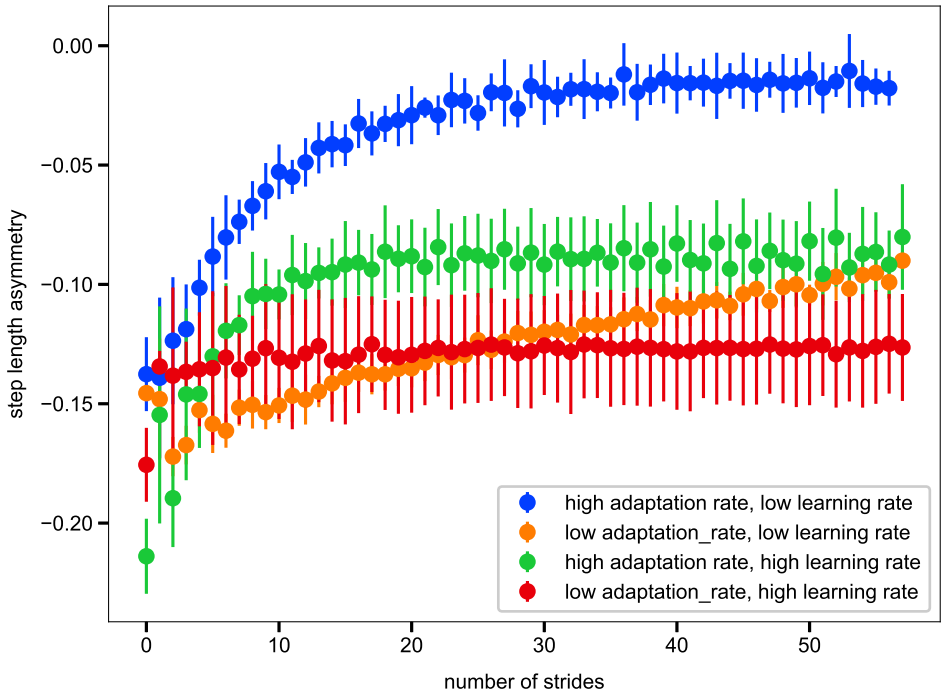

Fig 8. Step length asymmetries for different adaptation and learning rates. The values are averaged over three 80 s simulations for each combination of adaptation and learning rates. The bars represent the standard deviation.

Discussion

In this study, we showed that a commonly used spinal reflex model is capable of handling continuous perturbations introduced by a split-belt treadmill running at a 2:1 belt-speed ratio. However, a spinal gait controller alone cannot replicate the slow adaptations observed in human experiments. When extended with a physiological model of the cerebellum, which captures its main functions of sensorimotor prediction and error processing, the model exhibited adaptation patterns similar to humans, even though the cerebellum model only adjusted the timing of the liftoff phase. Specifically, the SLA converged from an initially asymmetric level toward symmetry, driven primarily by adjustments in the fast step length. The adaptation of SLA emerged from changes in both spatial and temporal domains, with temporal adaptations occurring at a faster rate. The joint kinematics remained similar throughout the adaptation period.

Our experiments indicate that step length symmetry can be modulated without an adaptation of reflex gains. This finding complements the findings of Refy et al. [36], who suggest that adapting spinal reflexes can drive changes in gait asymmetry. It is important to acknowledge that, in natural walking, individuals likely adapt both reflex gains and thresholds over time. However, our study highlights the isolated effect of modulating only the timing of phases within the gait cycle.

We found that modulating the timing of the liftoff threshold resulted in a temporal

adaptation, characterized by a reduction in the phase lag of the fast limb relative to the slow limb, but also in a spatial adaptation, characterized by a reduction in the center of oscillation difference. The change in the temporal domain occurred faster than the change in the spatial domain, which corresponds to what has been found in human experiments [18]. In literature, these different adaptation rates have led to the hypothesis that there may be separate neural mechanisms for spatial and temporal locomotor adjustments. Our findings suggest that the same neural mechanism (in our case the adaptation of the liftoff threshold) can be responsible for spatial and temporal adaptations at different time scales.

Our investigation of high versus low adaptation rates corresponded to the step length adaptation curves of fast and slow adapters described in [61]. In addition, the investigation of different learning rates leads to new hypotheses about motor adaptations in split-belt walking. We might infer that persons, for which the cerebellum adapts its internal model faster (corresponding to a high learning rate) tolerate a higher level of SLA. This implies that they converge to a steady-state level of greater asymmetry during split-belt walking compared to those with a slower internal model update (low learning rate). This hypothesis should be investigated by future studies or experiments. Another question that arises and should further be investigated is if the update rate of the cerebellar prediction and the update rate of motor commands are actually separable in humans and can be modulated or trained independently, or if they are inherently linked.

The joint kinematics of our model displayed some deviations from those observed in human subjects, such as an increased hip flexion during the swing phase in both legs and a greater range of motion in the ankle of the slow leg. We attribute these differences to the design of the reflex controller, suggesting that its configuration may not be ideally suited for split-belt treadmill walking. However, the deviations do not affect our primary findings. Our focus was on the changes in gait parameters between the start and end of the adaptation period and the integration of the cerebellum model, rather than the tuning of the spinal reflex controller. Thus, the key result for the kinematics is that they remain consistent throughout the simulation despite the change in SLA, like in human experiments. This underscores the functionality of our cerebellum model.

The exact mechanisms of the cerebellum in motor adaptations are a topic of ongoing research. We aimed to keep our cerebellum model as simple as possible while preserving its key functions. To this end, we used a single error metric — specifically, the difference between a predicted and the actual SLA. Based on this error, both the left and right legs were adapted according to their respective gradients. This approach produced realistic step length adaptation curves in which the fast leg showed greater adaptation than the slow leg. However, separate control circuits or error metrics may exist for the left and right leg. For example, Fujiki et al. [34] proposed a time-based error function for the left and the right limb. Another possibility is that the error might relate to the difference between the current walking pattern and the energetically optimal step frequencies, along with the corresponding stance and swing times, that humans would naturally adopt if the treadmill belts ran symmetrically at each of the two different speeds. Malone et al. [49] even proposed different error metrics for spatial and temporal adaptations. Yet again, individual control circuits cannot be isolated in human experiments. While we ran our experiments with a simple error function, our framework can be used to computationally test different error metrics or control hypotheses in future studies.

To allow the model to adjust the phasing between the limbs under asymmetric conditions, we introduced an additional threshold to indicate the start of the liftoff phase, rather than relying on the HS of the contralateral leg to trigger it. The temporal decomposition revealed that this approach was effective, although the phase difference

between limbs was smaller than observed in experiments. In our model, this threshold was time-based, meaning liftoff occurred at a fixed time after HS. While we cannot be certain that this mechanism reflects the actual biological trigger for liftoff, we saw from our experimental measurement that this aspect of gait timing is also modifiable. Another approach could have been to trigger liftoff based on the distance between the trailing (or leading) foot and the pelvis, indicating that liftoff would occur when the leg reaches a specific angle, or when the COM is near the base of support when the trailing leg lifts off. However, we eventually chose the time-based threshold, as it in the broadest sense inspired by the rhythmic nature of central pattern generators, known for coordinating phase transitions and being modifiable by supraspinal input [62, 63].

Our neuromusculoskeletal model was a reflex model that is frequently used in literature and has demonstrated robustness against other types of perturbations. However, different models could be better suited for the investigation of specific aspects of motor adaptation in split-belt walking. For example, Malone et al. [49] have suggested that adaptations in the spatial domain are a consequence of modulating foot placement. Active foot placement is not possible with our spinal reflex model though. Song and Geyer [33] have proposed a neuromusculoskeletal model with an additional supraspinal control structure that adjusts the desired foot placements and could serve as an alternative to our approach of adapting the start of the liftoff phase. Furthermore, there are indications that CPGs might contribute to the spinal control of locomotion [64]. CPGs are neural circuits that generate rhythmic motor patterns without the need for sensory feedback. These circuits have been integrated into neuromusculoskeletal models both on top [65] or instead of [30] reflex-based neural circuits. Such models could help explore whether the phase-resetting approach proposed by Aoi et al. [35] - originally developed for a torque-controlled robot to replicate fast and slow gait adaptations - can be generalized to a neuromusculoskeletal model. Nevertheless, our results demonstrate that even a basic reflex model is sufficient for walking on a split-belt treadmill and for capturing salient features of slow and fast adaptations.

The objective function that we chose incorporated different aspects relevant for human gait. However, we cannot be certain that these terms are equally relevant for split-belt walking. It is known that objective functions vary with speed [66], it is thus likely that different terms may play a role in split-belt walking as well. It was for example shown that pure energy minimization would lead to a large positive SLA (up to 0.42) [23]. Even though it has been shown that after prolonged split-belt walking people learn to exploit the assistance from the treadmill to reduce metabolic cost, such high positive SLAs have not been observed experiments and might indicate that additional factors are involved [23, 67]. Darter et al. [68] have also shown that maintaining stability against the continuous perturbation induced by the two belt speeds is relevant in split-belt walking. In our case, stability was indirectly incorporated into the objective function through an upper-level objective that ensured the model could complete the entire simulation period without falling, before other objective terms became relevant. It is also likely that the objectives that humans rely on change within the course of the intervention, with a high focus on stability at the beginning that becomes less over time while the relative influence of other factors increases. Westermann et al. [69] used a time-varying objective function in their inverse optimal control simulations of jumping to determine the relative influence of the different terms over time. A similar approach could be used to identify the relevance of different objective terms in split-belt walking including motor adaptations.

In this work, we focused on the slow adaptations that occur while the treadmill is running at two different belt speeds, and did not take into account the after-effects that happen when the belts are running again at the same speed. We therefore started with an initial guess that already incorporated the reactive changes that occur immediately

when the belt speeds are made asymmetric. Future work could extend the study and also include the transitions from and to symmetric belt speeds. It has been shown that proprioception, as well as the perception of belt speed, play a role in this fast adaptation process [70]. However, neither of these two factors is accounted for in our model. We could thus think about how to include more sensory inputs or even psychological processes in control models.

Conclusion

We extended a reflex model with a supraspinal structure representing a physiological model of the cerebellum that incorporated the key functions of error computation and sensorimotor adaptation. In our case, we allowed the cerebellum to adapt only the timing-related start of the liftoff phase of the spinal controller, since an isolated adaptation of specific parameters is not feasible in experimental studies. We showed that a reflex model is capable of walking on a split-belt treadmill with the belts running at a 2:1 beltspeed ratio. When extended by the cerebellum model, the reflex model demonstrated slow adaptation patterns that are also observed in human experiments. Specifically, we observed a decrease in SLA, characterized by adaptations in both the spatial and temporal domains. In our simulations, as in human experiments, the fast leg contributed more to the change in SLA, even though the adaptation rate parameter of our cerebellum model was the same for both the left and right legs. The model also reproduced adaptation patterns similar to those of slow and fast learners by adjusting only one parameter: the adaptation rate of our cerebellum model. No adaptations were present when we used the model without the cerebellum. Our study showed that reflex gains do not necessarily need to be adapted to achieve an adaptation of SLA. Eventually, our simulations suggest that the same neural process might be responsible for temporal and spatial adaptations at different rates. Our neuromusculoskeletal simulations enable a better understanding of individual processes of motor adaptations. Our framework supports dynamic adaptation of control parameters and can be expanded to test additional motor control hypotheses.

Supporting information

S1 File. Details on the experimental data and parameter computation.

S2 Video. Video of one representative split-belt walking simulations at 2:1 belt speed ratio with adaptations driven by the cerebellum model.

S3 Video. Video of one representative split-belt walking simulations at 2:1 belt speed ratio without adaptations driven by the cerebellum model

Acknowledgments

This work was funded by the Deutsche Forschungsgemeinschaft (DFG, German Research Foundation) – SFB 1483 – Project-ID 442419336, EmpkinS. We thank Thomas Geijtenbeeck for his support with SCONE and Hyfydy.

References

1. Severini G, Zych M. Locomotor adaptations: paradigms, principles and perspectives. Progress in Biomedical Engineering. 2022;4(4):042003. doi:10.1088/2516-1091/ac91b6 .

2. Weerdesteyn V, Hollands KL, Hollands MA. Chapter 8 - Gait adaptability. In: Day BL, Lord SR, editors. Balance, Gait, and Falls. vol. 159 of Handbook of Clinical Neurology. Elsevier; 2018. p. 135–146.

3. McCrum C, Gerards MHG, Karamanidis K, Zijlstra W, Meijer K. A systematic review of gait perturbation paradigms for improving reactive stepping responses and falls risk among healthy older adults. European review of aging and physical activity. 2017;14:3. doi:10.1186/s11556-017-0173-7 .

4. Lam T, Anderschitz M, Dietz V. Contribution of feedback and feedforward strategies to locomotor adaptations. Journal of neurophysiology. 2006;95(2):766–773. doi:10.1152/jn.00473.2005 .

5. Helm EE, Reisman DS. The Split-Belt Walking Paradigm: Exploring Motor Learning and Spatiotemporal Asymmetry Poststroke. Physical medicine and rehabilitation clinics of North America. 2015;26(4):703–713. doi:10.1016/j.pmr.2015.06.010 .

6. Reisman DS, Block HJ, Bastian AJ. Interlimb coordination during locomotion: what can be adapted and stored? Journal of neurophysiology. 2005;94(4):2403–2415. doi:10.1152/jn.00089.2005 .

7. Reisman DS, Wityk R, Silver K, Bastian AJ. Locomotor adaptation on a split-belt treadmill can improve walking symmetry post-stroke. Brain : a journal of neurology. 2007;130(Pt 7):1861–1872. doi:10.1093/brain/awm035 .

8. Yokoyama H, Sato K, Ogawa T, Yamamoto SI, Nakazawa K, Kawashima N. Characteristics of the gait adaptation process due to split-belt treadmill walking under a wide range of right-left speed ratios in humans. PloS one. 2018;13(4):e0194875. doi:10.1371/journal.pone.0194875 .

9. Buurke TJW, Lamoth CJC, Vervoort D, van der Woude LHV, den Otter R. Adaptive control of dynamic balance in human gait on a split-belt treadmill. The Journal of experimental biology. 2018;221(Pt 13). doi:10.1242/jeb.174896 .

10. Hoogkamer W, Bruijn SM, Potocanac Z, van Calenbergh F, Swinnen SP, Duysens J. Gait asymmetry during early split-belt walking is related to perception of belt speed difference. Journal of neurophysiology. 2015;114(3):1705–1712. doi:10.1152/jn.00937.2014 .

11. Morton SM, Bastian AJ. Cerebellar contributions to locomotor adaptations during splitbelt treadmill walking. The Journal of neuroscience : the official journal of the Society for Neuroscience. 2006;26(36):9107–9116. doi:10.1523/JNEUROSCI.2622-06.2006 .

12. Hinton DC, Conradsson DM, Paquette C. Understanding Human Neural Control of Short-term Gait Adaptation to the Split-belt Treadmill. Neuroscience. 2020;451:36–50. doi:10.1016/j.neuroscience.2020.09.055 .

13. Welniarz Q, Worbe Y, Gallea C. The Forward Model: A Unifying Theory for the Role of the Cerebellum in Motor Control and Sense of Agency. Frontiers in Systems Neuroscience. 2021;15:644059. doi:10.3389/fnsys.2021.644059 .

14. Bastian AJ. Understanding sensorimotor adaptation and learning for rehabilitation. Current opinion in neurology. 2008;21(6):628–633. doi:10.1097/WCO.0b013e328315a293 .

15. Shadmehr R, Smith MA, Krakauer JW. Error correction, sensory prediction, and adaptation in motor control. Annual review of neuroscience. 2010;33:89–108. doi:10.1146/annurev-neuro-060909-153135 .

16. Tseng YW, Diedrichsen J, Krakauer JW, Shadmehr R, Bastian AJ. Sensory prediction errors drive cerebellum-dependent adaptation of reaching. Journal of neurophysiology. 2007;98(1):54–62. doi:10.1152/jn.00266.2007 .

17. Finley JM, Long A, Bastian AJ, Torres-Oviedo G. Spatial and Temporal Control Contribute to Step Length Asymmetry During Split-Belt Adaptation and Hemiparetic Gait. Neurorehabilitation and neural repair. 2015;29(8):786–795. doi:10.1177/1545968314567149 .

18. Malone LA, Bastian AJ. Thinking about walking: effects of conscious correction versus distraction on locomotor adaptation. Journal of neurophysiology. 2010;103(4):1954–1962. doi:10.1152/jn.00832.2009 .

19. Gonzalez-Rubio M, Velasquez NF, Torres-Oviedo G. Explicit Control of Step Timing During Split-Belt Walking Reveals Interdependent Recalibration of Movements in Space and Time. Frontiers in human neuroscience. 2019;13:207. doi:10.3389/fnhum.2019.00207 .

20. Iturralde PA, Torres-Oviedo G. Corrective Muscle Activity Reveals Subject-Specific Sensorimotor Recalibration. eNeuro. 2019;6(2). doi:10.1523/ENEURO.0358-18.2019 .

21. MacLellan MJ, Ivanenko YP, Massaad F, Bruijn SM, Duysens J, Lacquaniti F. Muscle activation patterns are bilaterally linked during split-belt treadmill walking in humans. Journal of neurophysiology. 2014;111(8):1541–1552. doi:10.1152/jn.00437.2013 .

22. Kambic RE, Roemmich RT, Bastian AJ. Joint-level coordination patterns for split-belt walking across different speed ratios. Journal of neurophysiology. 2023;129(5):969–983. doi:10.1152/jn.00323.2021 .

23. Price M, Huber ME, Hoogkamer W. Minimum effort simulations of split-belt treadmill walking exploit asymmetry to reduce metabolic energy expenditure. Journal of neurophysiology. 2023;129(4):900–913. doi:10.1152/jn.00343.2022 .

24. Muñoz D, de Marchis C, Gizzi L, Severini G. Predictive simulation of sit-to-stand based on reflexive-controllers. PLOS ONE. 2022;17(12):e0279300. doi:10.1371/journal.pone.0279300 .

25. de Groote F, Falisse A. Perspective on musculoskeletal modelling and predictive simulations of human movement to assess the neuromechanics of gait. Proceedings Biological sciences. 2021;288(1946):20202432. doi:10.1098/rspb.2020.2432 .

26. Song S, Geyer H. Evaluation of a Neuromechanical Walking Control Model Using Disturbance Experiments. Frontiers in computational neuroscience. 2017;11:15. doi:10.3389/fncom.2017.00015 .

27. Bunz EK, Haeufle DFB, Remy CD, Schmitt S. Bioinspired preactivation reflex increases robustness of walking on rough terrain. Scientific reports. 2023;13(1):13219. doi:10.1038/s41598-023-39364-3 .

28. Haeufle DFB, Schmortte B, Geyer H, Müller R, Schmitt S. The Benefit of Combining Neuronal Feedback and Feed-Forward Control for Robustness in Step Down Perturbations of Simulated Human Walking Depends on the Muscle Function. Frontiers in computational neuroscience. 2018;12:80. doi:10.3389/fncom.2018.00080 .

29. Ong CF, Geijtenbeek T, Hicks JL, Delp SL. Predicting gait adaptations due to ankle plantarflexor muscle weakness and contracture using physics-based musculoskeletal simulations. PLoS Computational Biology. 2019;15(10):e1006993. doi:10.1371/journal.pcbi.1006993 .

30. Di Russo A, Stanev D, Sabnis A, Danner SM, Ausborn J, Armand S, et al. Investigating the roles of reflexes and central pattern generators in the control and modulation of human locomotion using a physiologically plausible neuromechanical model. bioRxiv. 2023; p. 2023.01.25.525432. doi:10.1101/2023.01.25.525432 .

31. Veerkamp K, Waterval NFJ, Geijtenbeek T, Carty CP, Lloyd DG, Harlaar J, et al. Evaluating cost function criteria in predicting healthy gait. Journal of Biomechanics. 2021;123:110530. doi:10.1016/j.jbiomech.2021.110530 .

32. Ramadan R, Meischein F, Reimann H. High-level motor planning allows flexible walking at different gait patterns in a neuromechanical model. Frontiers in bioengineering and biotechnology. 2022;10:959357. doi:10.3389/fbioe.2022.959357 .

33. Song S, Geyer H. A neural circuitry that emphasizes spinal feedback generates diverse behaviours of human locomotion. The Journal of Physiology. 2015;593(16):3493–3511. doi:10.1113/JP270228 .

34. Fujiki S, Aoi S, Funato T, Tomita N, Senda K, Tsuchiya K. Adaptation mechanism of interlimb coordination in human split-belt treadmill walking through learning of foot contact timing: a robotics study. Journal of the Royal Society, Interface. 2015;12(110):0542. doi:10.1098/rsif.2015.0542 .

35. Aoi S, Amano T, Fujiki S, Senda K, Tsuchiya K. Fast and Slow Adaptations of Interlimb Coordination via Reflex and Learning During Split-Belt Treadmill Walking of a Quadruped Robot. Frontiers in robotics and AI. 2021;8:697612. doi:10.3389/frobt.2021.697612 .

36. Refy O, Mo O, Hsu J, Weber DJ, Geyer H. Changes in Gait Asymmetry May Be Caused by Adaptation of Spinal Reflexes. bioRxiv. 2024;doi:10.1101/2024.02.04.578817 .

37. Geyer H, Herr H. A muscle-reflex model that encodes principles of legged mechanics produces human walking dynamics and muscle activities. IEEE transactions on neural systems and rehabilitation engineering : a publication of the IEEE Engineering in Medicine and Biology Society. 2010;18(3):263–273. doi:10.1109/TNSRE.2010.2047592 .

38. Geijtenbeek T. SCONE: Open Source Software for Predictive Simulation of Biological Motion. Journal of Open Source Software. 2019;4(38):1421. doi:10.21105/joss.01421 .

39. Geijtenbeek T. The Hyfydy Simulation Software; 2021. Available from: `https://hyfydy.com`.

40. Delp SL, Loan JP, Hoy MG, Zajac FE, Topp EL, Rosen JM. An interactive graphics-based model of the lower extremity to study orthopaedic surgical procedures. IEEE transactions on bio-medical engineering. 1990;37(8):757–767. doi:10.1109/10.102791 .

41. Rajagopal A, Dembia CL, DeMers MS, Delp DD, Hicks JL, Delp SL. Full-Body Musculoskeletal Model for Muscle-Driven Simulation of Human Gait. IEEE transactions on bio-medical engineering. 2016;63(10):2068–2079. doi:10.1109/TBME.2016.2586891 .

42. Millard M, Uchida T, Seth A, Delp SL. Flexing Computational Muscle: Modeling and Simulation of Musculotendon Dynamics. Journal of Biomechanical Engineering. 2013;135(2):021005. doi:10.1115/1.4023390 .

43. Hunt KH, Crossley FRE. Coefficient of Restitution Interpreted as Damping in Vibroimpact. Journal of Applied Mechanics. 1975;42(2):440–445. doi:10.1115/1.3423596 .

44. Di Russo A, Stanev D, Armand S, Ijspeert A. Sensory modulation of gait characteristics in human locomotion: A neuromusculoskeletal modeling study. PLoS computational biology. 2021;17(5):e1008594. doi:10.1371/journal.pcbi.1008594 .

45. Zehr EP, Stein RB. What functions do reflexes serve during human locomotion? Progress in Neurobiology. 1999;58(2):185–205. doi:https://doi.org/10.1016/S0301-0082(98)00081-1 .

46. Ong CF, Geijtenbeek T, Hicks JL, Delp SL. Predicting gait adaptations due to ankle plantarflexor muscle weakness and contracture using physics-based musculoskeletal simulations. PLoS Computational Biology. 2019;15(10):e1006993. doi:10.1371/journal.pcbi.1006993 .

47. Bruel A, Ghorbel SB, Di Russo A, Stanev D, Armand S, Courtine G, et al. Investigation of neural and biomechanical impairments leading to pathological toe and heel gaits using neuromusculoskeletal modelling. The Journal of Physiology. 2022;600(11):2691–2712. doi:10.1113/JP282609 .

48. Popa LS, Ebner TJ. Cerebellum, Predictions and Errors. Frontiers in Cellular Neuroscience. 2019;12. doi:10.3389/fncel.2018.00524 .

49. Malone LA, Bastian AJ, Torres-Oviedo G. How does the motor system correct for errors in time and space during locomotor adaptation? Journal of neurophysiology. 2012;108(2):672–683. doi:10.1152/jn.00391.2011 .

50. Thoroughman KA, Shadmehr R. Learning of action through adaptive combination of motor primitives. Nature. 2000;407(6805):742–747. doi:10.1038/35037588 .

51. Wang JM, Hamner SR, Delp SL, Koltun V. Optimizing locomotion controllers using biologically-based actuators and objectives. ACM Trans Graph. 2012;31(4). doi:10.1145/2185520.2185521 .

52. Dorn TW, Wang JM, Hicks JL, Delp SL. Predictive simulation generates human adaptations during loaded and inclined walking. PloS one. 2015;10(4):e0121407. doi:10.1371/journal.pone.0121407 .

53. Hansen N, Müller SD, Koumoutsakos P. Reducing the Time Complexity of the Derandomized Evolution Strategy with Covariance Matrix Adaptation (CMA-ES). Evolutionary Computation. 2003;11(1):1–18. doi:10.1162/106365603321828970 .

54. Lassmann C, Ilg W, Rattay TW, et al. Dysfunctional neuro-muscular mechanisms explain gradual gait changes in prodromal spastic paraplegia. Journal of NeuroEngineering and Rehabilitation. 2023;20(90). doi:10.1186/s12984-023-01206-8 .

55. Waterval NFJ, Veerkamp K, Geijtenbeek T, Harlaar J, Nollet F, Brehm MA, et al. Validation of forward simulations to predict the effects of bilateral plantarflexor weakness on gait. Gait & Posture. 2021;87:33–42. doi:https://doi.org/10.1016/j.gaitpost.2021.04.020 .

56. Choi JT, Bastian AJ. Adaptation reveals independent control networks for human walking. Nature Neuroscience. 2007;10(8):1055 – 1062.

57. Brinkerhoff S, Sánchez N, Roper J. Habitual exercise evokes fast and persistent adaptation during split-belt walking. PLOS ONE. 2023;18:e0286649. doi:10.1371/journal.pone.0286649 .

58. Sombric CJ, Torres-Oviedo G. Augmenting propulsion demands during split-belt walking increases locomotor adaptation of asymmetric step lengths. Journal of NeuroEngineering and Rehabilitation. 2020;17(1):69. doi:10.1186/s12984-020-00698-y .

59. Sombric C, Calvert J, Torres-Oviedo G. Large Propulsion Demands Increase Locomotor Adaptation at the Expense of Step Length Symmetry. Frontiers in Physiology. 2019;10. doi:10.3389/fphys.2019.00060 .

60. Tesio L, Malloggi C, Malfitano C, Coccetta CA, Catino L, Rota V. Limping on split-belt treadmills implies opposite kinematic and dynamic lower limb asymmetries. International Journal of Rehabilitation Research. 2018;41(4):304–315. doi:10.1097/MRR.0000000000000320 .

61. Jacobsen NA, Ferris DP. Exploring Electrocortical Signatures of Gait Adaptation: Differential Neural Dynamics in Slow and Fast Gait Adapters. eNeuro. 2024;11(7). doi:10.1523/ENEURO.0515-23.2024 .

62. Daun S, Rubin JE, Rybak IA. Control of oscillation periods and phase durations in half-center central pattern generators: a comparative mechanistic analysis. Journal of Computational Neuroscience. 2009;27(1):3–36. doi:10.1007/s10827-008-0124-4 .

63. MacKay-Lyons M. Central Pattern Generation of Locomotion: A Review of the Evidence. Physical Therapy. 2002;82(1):69–83. doi:10.1093/ptj/82.1.69 .

64. Minassian K, Hofstoetter US, Dzeladini F, Guertin PA, Ijspeert A. The Human Central Pattern Generator for Locomotion: Does It Exist and Contribute to Walking? The Neuroscientist. 2017;23(6):649–663. doi:10.1177/1073858417699790 .

65. Dzeladini F, van den Kieboom J, Ijspeert A. The contribution of a central pattern generator in a reflex-based neuromuscular model. Frontiers in human neuroscience. 2014;8:371. doi:10.3389/fnhum.2014.00371 .

66. Weng J, Hashemi E, Arami A. Human Gait Cost Function Varies With Walking Speed: An Inverse Optimal Control Study. IEEE Robotics and Automation Letters. 2023;8(8):4777–4784. doi:10.1109/LRA.2023.3289088 .

67. Sánchez N, Simha SN, Donelan JM, Finley JM. Using asymmetry to your advantage: learning to acquire and accept external assistance during prolonged split-belt walking. Journal of neurophysiology. 2021;125(2):344–357. doi:10.1152/jn.00416.2020 .

68. Darter BJ, Labrecque BA, Perera RA. Dynamic stability during split-belt walking and the relationship with step length symmetry. Gait & Posture. 2018;62:86–91. doi:https://doi.org/10.1016/j.gaitpost.2018.03.006 .

69. Westermann K, Lin JFS, Kulić D. Inverse optimal control with time-varying objectives: application to human jumping movement analysis. Scientific Reports. 2020;10(1):11174. doi:10.1038/s41598-020-67901-x .

70. Vazquez A, Statton MA, Busgang SA, Bastian AJ. Split-belt walking adaptation recalibrates sensorimotor estimates of leg speed but not position or force. Journal of Neurophysiology. 2015;114(6):3255–3267. doi:10.1152/jn.00302.2015 .